

Roel Moonen<sup>1,\*</sup>  
Jeroen Alles<sup>2</sup>  
Erik-jan Ras<sup>1</sup>  
Clare Harvey<sup>1</sup>  
Jacob A. Moulijn<sup>3</sup>

# Performance Testing of Hydrodesulfurization Catalysts Using a Single-Pellet-String Reactor

*Dedicated to Professor Rüdiger Lange on the occasion of his 65th birthday*

Small-scale parallel trickle-bed reactors were used to evaluate the performance of a commercial hydrodesulfurization catalyst under industrially relevant conditions. Catalyst extrudates were loaded as a single string in reactor tubes. It is demonstrated that product sulfur levels and densities obtained with the single-pellet-string reactor are close to the results obtained in a bench-scale fixed-bed reactor operated under the same conditions. Moreover, parallel single-pellet-string reactors show high reproducibility. To study the hydrodynamic effects of the catalyst-bed packing, the catalyst-bed length was varied by loading different amounts of catalysts, and crushed catalyst was also loaded.

**Keywords:** Catalysts, Fixed bed, Hydrodesulfurization, Reactors, Single-Pellet String

*Received:* February 24, 2017; *revised:* April 11, 2017; *accepted:* July 06, 2017

**DOI:** 10.1002/ceat.201700098

© 2017 The Authors. Published by Wiley-VCH Verlag GmbH & Co. KGaA. This is an open access article under the terms of the Creative Commons Attribution License, which permits use, distribution and reproduction in any medium, provided the original work is properly cited.

## 1 Introduction

The hydrodesulfurization (HDS) of gasoil is one of the key processes in refineries that enables them to meet the product properties as demanded by the market [1,2]. The HDS process should produce diesel with the target sulfur levels while meeting important product properties such as density, cetane index, and cold-flow properties. Hydrogen consumption is another important parameter as the hydrogen availability is often limited. Refineries have a need for catalysts that are flexible in terms of acceptable feedstocks; blends such as straight-run gas oil (SRGO) and light cycle oil (LCO) need to be converted without sacrificing catalyst lifetime or product properties. Moreover, the feedstock converted is often changed over time, depending on availability and cost. The typical reaction occurring in the hydrodesulfurization of diesel-like feedstocks is shown in Fig. 1.

The lifetime that is required for a hydrotreating catalyst is in the order of magnitude of multiple years depending on the severity of the conditions [3]. Catalyst manufacturers need to maintain a continuous effort in catalyst development to keep up with or stay ahead of their competitors and to simply deal with the ever changing landscape of refinery operations. For this purpose, relevant and scalable test data is required. The test results obtained in the laboratory should be meaningful and be able to predict the performance of commercial-scale reactors.

Catalyst evaluation is an important step in optimizing catalytic processes with respect to the product yield, energy efficiency, and overall product quality. Historically, the performance of heterogeneous catalysts has been evaluated by using

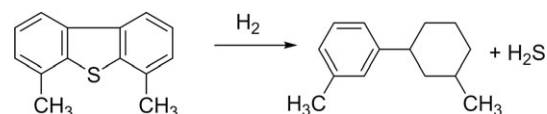


**Figure 1.** Typical reaction occurring in the hydrodesulfurization of diesel-like feedstocks. Note that both desulfurization and hydrogenation take place.

bench-scale reactor systems. These reactor volumes typically vary between 100 and 300 mL. In recent years, there has been a clear trend towards small laboratory reactors, sometimes with catalyst volumes as low as 1 mL (e.g., the reactor system used in this study). Some of the obvious advantages of downsizing are the reduced cost of construction and operation. Reactors of smaller scale are typically more ideal in terms of heat flow and hydrodynamics than larger reactors and therefore provide data that are intrinsically easier to translate to an industrial scale

<sup>1</sup>Roel Moonen, Dr. Erik-jan Ras, Dr. Clare Harvey  
Roel.moonen@avantium  
Avantium Chemicals, Zekeringstraat 29, 1014BV Amsterdam, The Netherlands.

<sup>2</sup>Jeroen Alles  
Albemarle Catalysts, Nieuwendammerkade 1–3, 1022AB Amsterdam, The Netherlands.

<sup>3</sup>Dr. Jacob A. Moulijn  
Delft University of Technology, Faculty of Applied Sciences, Catalysis Engineering, Chemical Engineering Department, Van der Maasweg 9, 2629 HZ Delft, The Netherlands.

[4]. Smaller reactors are especially beneficial for parallel reactor systems. Parallel testing allows for replication – determination of the statistical significance of the results obtained – and for simply evaluating more catalyst options at the same time. In addition, smaller volumes reduce the amount of chemicals required and consequently reduce the amount of waste materials produced. Reduced feedstock requirements also avoid the typical issues associated with obtaining large quantities of such feedstocks, such as handling, shipping, and storage (for longer-term availability of reference feed material). In addition, the safety risks are reduced relative to operation of larger reactors and the effective use of laboratory floor space (small footprint) is enhanced. Overall, small-scale parallel reactor systems like the unit described in this paper are more cost effective than their large-scale counterparts.

Various authors have reported work on hydrotreating using bench-scale reactors [5]. The typical bench-scale reactor has a diameter of 1.2–2.5 cm and a catalyst bed length of 30–80 cm. The use of bench-scale reactors requires careful packing of the extrudates in the reactor tube and many authors concluded that fine inert diluent needs to be loaded into the reactor to improve the plug-flow behavior, avoid wall effects, and guarantee good catalyst wetting. Although reproducible packing of bench-scale reactors can be achieved, the packing needs to be done in a well-controlled manner to avoid uneven distribution of the extrudates and large voids, which result in maldistribution of the gas and liquid flow in the bench-scale reactor [7]. The oil feed needs to be well distributed at the entrance of the reactor to avoid partial wetting of the catalyst bed due to preferential flow patterns.

Laboratory reactors are operated at a significantly lower fluid velocity than their industrial-scale counterparts. When operated at equal space velocity, the superficial gas and liquid velocity is a factor of 20–100 times lower. It should be noted that reducing the superficial fluid velocity and reactor diameter can have an impact on the hydrodynamics of the trickle-flow reactor. Proper plug flow and catalyst wetting is required to avoid the influence of hydrodynamics on the obtained test results [8]. Kallinikos and Papayannakos [9] suggested the use of a spiral reactor with a diameter only slightly larger than the catalyst extrudates. This type of reactor offers the advantage of lower quantities of catalyst and oil feed, excellent temperature control, and reproducible reactor loading due to the single extrudates in the diameter of the reactor. The reactors were 2.1 mm in diameter, and the catalyst size was only slightly smaller than the reactor diameter. The authors [9] showed that there is negligible impact of the reactor length (varied between 2 to 6 m) on the HDS reaction rate when using this type of reactor.

In the research presented herein, a single string of extrudates was loaded in straight reactor tubes with an internal diameter of 2 mm and a catalyst-bed length of up to 30 cm. A variety of reactor-loading methodologies was tested, and their performance for HDS was evaluated in comparison to a bench-scale reactor.

## 2 Experimental Section

### 2.1 Bench-Scale Test Reactor

The bench-scale reactor was operated in up-flow mode and consisted of a reactor with an internal diameter of 20 mm and a catalyst-bed volume of 225 mL. The catalyst was tested as whole extrudates and was diluted with inert material. The temperature of the catalyst bed was measured by using multiple thermocouples inside the catalyst bed. The weight-average bed temperature (WABT) was determined from the average of the various temperatures measured inside the length of the reactor. The WABT is commonly used to summarize the temperature of a non-isothermal reactor. In this work, whenever the temperature of the large-scale reactor is referred to, WABT was used.

### 2.2 Single-Pellet-String Reactor

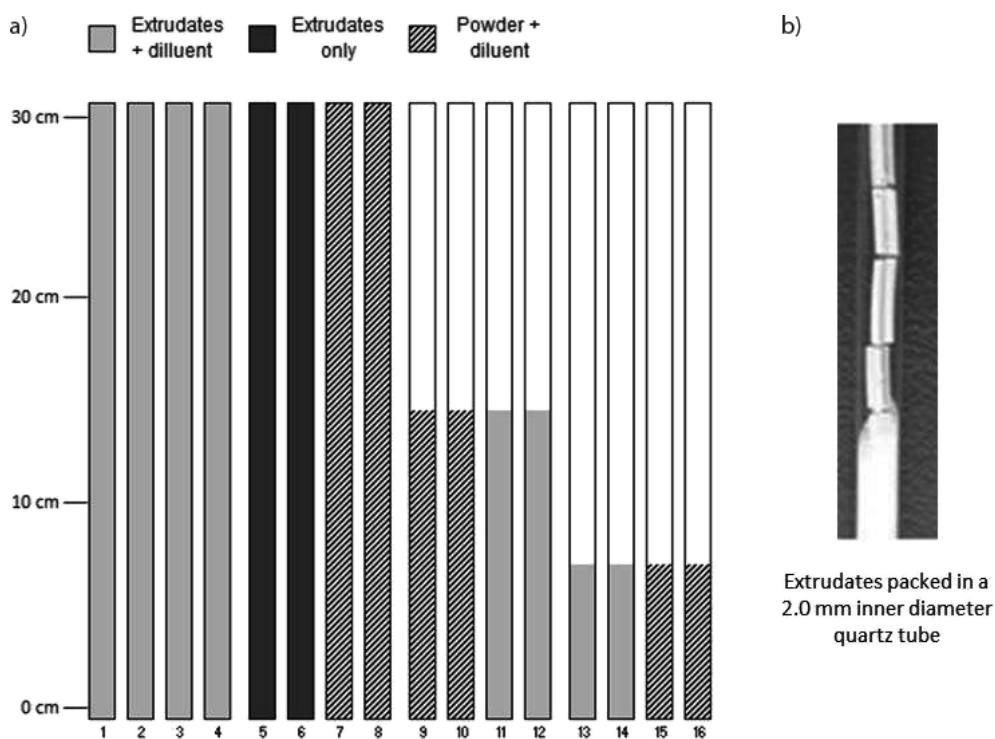
The single-pellet-string reactor was made of a stainless-steel tube with 2 mm inside diameter (ID) and contained a maximum catalyst-bed volume of 0.6 mL. The reactor tube was 55 cm, including a conditioning zone at the top of the reactor. Liquid was injected by using a capillary tube at the top of the reactor and hydrogen feed gas was concurrently flowing from top to bottom through the reactor tube.

Extrudates loaded in the reactor tubes automatically align as a string of extrudates (see Fig. 2). The use of a narrow reactor avoids any maldistribution of gas and liquid over the catalyst bed, thereby eliminating catalyst-bed channeling and incomplete wetting of the catalyst. The bed length of the extrudate string was varied between 7.5 and 30 cm. An inert diluent material was used as a filler for a selection of the beds with extrudates. This inert material (nonporous ceramic beads) with a diameter of 0.07 mm was added to the reactors after loading the extrudates. Gentle tapping of the tube distributes the inert material over the complete length of the reactor tube, thereby surrounding all extrudates.

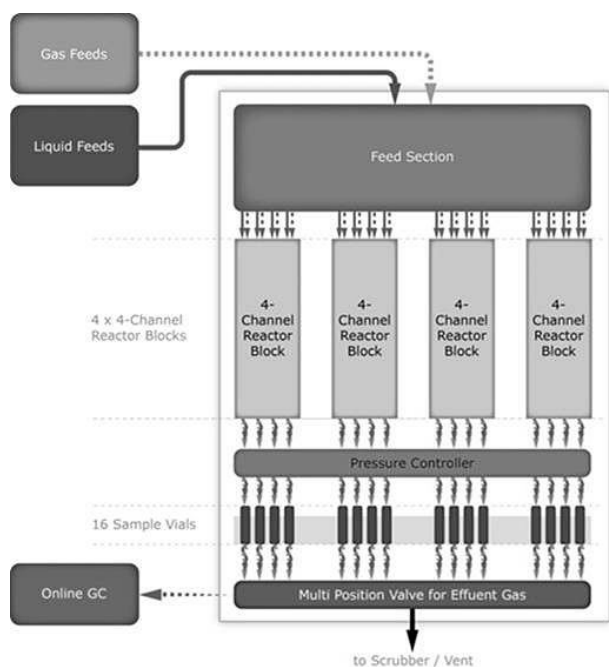
The reactor tubes were tested in a 16-parallel-reactor system, a commercially available “Flowrence” reactor system, as provided by Avantium B.V. [10]. To be able to operate reactors smaller than 1 mL, the Flowrence system contains various technical solutions to ensure stable and accurate control of gas, liquid, and pressure of each of the 16 parallel reactors. More information can be found in the corresponding patents [10–15].

Fig. 3 shows a schematic overview of the 16 parallel reactors. Hydrogen feed gas was distributed to 16 reactors, and the pressure of each channel was measured by using electronic pressure sensors. The oil feed was dosed by using a pump and was distributed to all 16 channels. The exact liquid flow rate of each of the individual liquid feed lines was measured and actively controlled to ensure even distribution of the oil feed to each of the reactors within 0.5 % relative standard deviation (RSD).

The reactor tubes were loaded into four separate heating blocks. The catalyst bed was loaded and placed within the isothermal zone. Each reactor block can be loaded with four reactor tubes, all operating at the same temperature. Each block



**Figure 2.** Schematic of the reactor loading for the 16 reactors used in this test (a) and an example of single-string packing (b). The reactors used during the test were made from stainless steel, with a total length of 50 cm. The maximum isothermal bed height in this case was 30 cm. An identical catalyst was tested in different bed volumes to achieve different *LHSV* values. The catalyst was tested as it is (in extrudate form) or crushed, and was tested when diluted with small particulate inert material surrounding the catalyst particles or without dilution.



**Figure 3.** Schematic representation of the reactor setup used [15]. The setup can be divided into four distinct sections: (1) feed section, in which gas and liquid feeds are distributed; (2) reactor section, containing four temperature blocks each holding four reactors; (3) pressure regulation, based on the principle of a back-pressure regulator; (4) effluent section, in which the heated and diluted reactor effluent was collected and analyzed. A more detailed description of each section and its workings is provided in the main text.

of four reactors can be operated at a chosen temperature without impact on the other heating blocks.

The reactor effluent, consisting of gas and liquid products, was diluted by using nitrogen gas and depressurized to atmospheric pressure. By dilution of nitrogen, the reactor effluent gas concentration was reduced, including hydrogen disulfide. This reduces recombination side effects under “ultra-low-sulfur-diesel” (ULSD) conditions. The diluted gas and liquid effluent can be sent to either a common waste outlet or to a set of 16 liquid collection vials. Liquid product was collected into 16 sample vials simultaneously while the gas was analyzed by online gas chromatography (GC).

The mass of the collected diesel product was determined by using a balance (XS104, Mettler Toledo), and was further analyzed for total sulfur (UV fluorescence Xplorer TSTN, TE instruments). For each of the collected diesel product samples, the gas phase (hydrogen and C1 to C4 hydrocarbons) was analyzed by GC (7890B, Agilent Technologies) using both thermal conductivity detector (TCD) and flame ionization detector (FID). The measured gas composition was used to calculate the hydrogen consumption and (light) gas yield. The liquid product density was determined by using a density meter (DM40, Mettler Toledo).

The test protocol for small-scale and bench-scale tests starts with an activation step. Straight-run gasoil feed doped with dimethyl disulfide was used for sulfurization of the catalyst. After this activation step, all catalysts were evaluated at a single operating pressure and the hydrogen-to-oil ratio through the complete length of the test run. Temperature was varied in three levels at 315, 325, and 335 °C, while the liquid hourly space velocity (*LHSV*) was varied from 0.44, 0.87, 1.75 to 3.50 h<sup>-1</sup>.

The bench-scale reactor was operated as a single reactor. The single-pellet-string reactor was operated with 16 reactors. All 16 parallel reactors were operated at the same process conditions for each condition of the test protocol.

### 2.3 Oil Feed and Catalyst

A commercial oil feed and catalyst were used for the work in this paper. The feed used was a blend of straight-run gas oil (SGRO) and light cycle oil (LCO). Tab.1 shows the most important properties of the feed. The catalyst was a commercial-grade NiMo HDS catalyst from Albemarle Corporation with extrudate (quadrolobe) sizes of 1.3 mm diameter and 3 to 5 mm length. Smaller catalysts were obtained after gentle crushing of the extrudates in a mortar (particle size 0.1–0.2 mm).

**Table 1.** Properties of the SRGO/LCO feed used in the tests.

Property	Value
Density [g mL <sup>-1</sup> ] at 15 °C	0.8787
Total sulfur [wt %]	1.5977
Total nitrogen [mg kg <sup>-1</sup> ]	440
Total aromatics [wt %]	48
<i>IBP</i> <sup>a</sup> / <i>FBP</i> <sup>b</sup> (ASTM D2887) [°C]	74/420

<sup>a</sup>*IBP* = initial boiling point; <sup>b</sup>*FBP* = final boiling point.

## 3 Results and Discussion

The comparability of the single-pellet-string reactor (SPSR) to a larger bench-scale reactor was investigated by studying a wide range of conditions. The sulfur content as a function of temperature and *LHSV* was compared, and modeling methods were used to confirm plug-flow behavior.

### 3.1 Single-Pellet-String Reactor Experiments

#### 3.1.1 Test Design and Raw Data

In a single experiment, different reactor loadings of the same catalyst were applied across 16 reactors. Variations in reactor loading included the use of unmodified extrudates and crushed extrudates, loading of extrudates with and without a surrounding inert diluent powder, and variations in bed volume. The full loading diagram for the experiment is shown in Fig.2. During the test, pressure and hydrogen-to-oil ratio were fixed, whereas temperature and *LHSV* were varied. At various stages of the test, test conditions were repeated to provide a check for any undesirable effects. The total duration

of the test was 570 h. The variations of temperature and *LHSV* executed during the test are shown in Fig. 4. It should be noted that the *LHSV* values shown only apply to those reactors containing a full catalyst bed (reactors 1–8). For the other reactors, containing smaller bed volumes, proportionally higher *LHSV* values were applied.

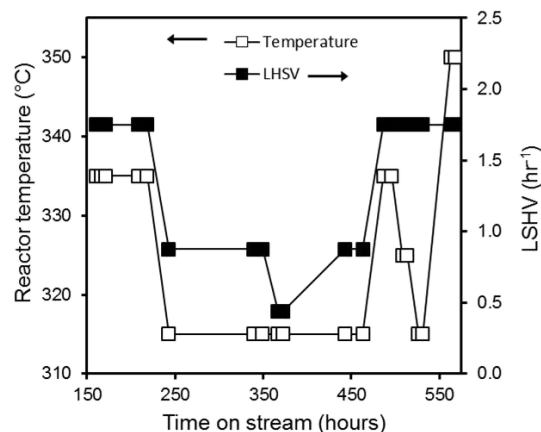


**Figure 4.** Temperature and *LHSV* program as executed as a function of time on stream. The first 150 h of the test comprised the catalyst pretreatment procedure (not shown here). No performance data was collected during this period. Markers indicate the measured values, the connecting lines serve as a guide to the eye.

The trends obtained from the single-pellet-string experiments are expected, with the sulfur content in the reaction product decreasing with increasing temperature. Likewise, the sulfur content of the reaction product decreases with decreasing space velocity as one would expect. These trends are shown in Fig. 5. Other key performance indicators recorded are hydrogen consumption and product density; the behavior of these is also as expected (not shown). Hydrogen consumption increases with increasing sulfur conversion. This is only partly due to the intended hydrodesulfurization reaction, and is also due to an increasing degree of hydrogenation of carbon-carbon double bonds present in the feedstock. Product density decreases with

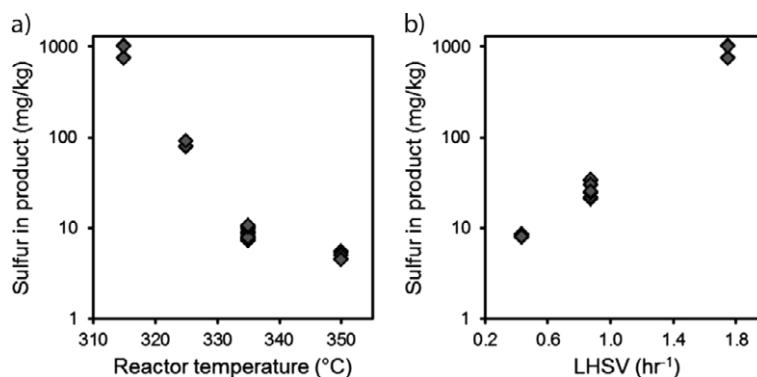


**Figure 5.** Sulfur mass fraction in the collected product as a function of temperature (a) at a constant *LHSV* of 1.75 h<sup>-1</sup> and as a function of *LHSV* (b) at a constant temperature of 315 °C. Note that the sulfur mass fraction is represented on a logarithmic scale to better highlight the trends in the data.



an increasing sulfur conversion, also due to partial saturation of the carbon-carbon double bonds.

### 3.1.2 Data Quality

In catalyst testing, regardless of the application or reactor scale, reproducibility of test results is always a key concern. For this test, reproducibility can easily be assessed by evaluating the data obtained for replicate catalyst loadings. The best point of comparison is the quadruplicate loading of a full catalyst bed in reactors 1–4 using extrudates combined with inert diluent, and the duplicate loading of extrudates without diluent in reactors 5 and 6 (Fig. 2). In Tab. 2, the sulfur content measured in these reactors is given for three different test temperatures.

**Table 2.** Sulfur content in the products recorded for replicate reactors at three different temperatures and with two different loading methods. In all cases, an  $LHSV$  of  $1.75\text{ h}^{-1}$  was applied.

Reactor	Sulfur in product [ $\text{mg kg}^{-1}$ ]		
	315 °C	325 °C	335 °C
<i>Extrudates + diluent</i>			
1	758	90.4	10.4
2	747	91.3	10.2
3	745	90.5	10.5
4	744	90.8	10.5
<i>Extrudates only</i>			
5	863	131	16.5
6	838	129	15.0

At first inspection, reproducibility of both the quadruplicate and duplicate is excellent. Especially under realistic target performance conditions (lower target sulfur levels), one cannot distinguish between reactors. This eliminates a key concern in catalyst testing: results are as reproducible as one could realistically expect. On taking a closer look, a significant difference is present between those reactors using diluent particles around the extrudates and those that do not. In all cases, a higher sulfur content is recorded in those reactors not using diluent (i.e., a lower sulfur conversion). This is in line with expectation, as the diluent is added to avoid catalyst bypassing.

The impact of the added diluent is best understood by comparing catalyst activity. A common means of doing this is to evaluate the temperature required ( $T_{\text{req}}$ ) to achieve a certain target sulfur level. In this case, the temperature required can be determined by simply applying first-order kinetics to the overall HDS reaction [16]. This transformation directly shows the impact of the added diluent. Those reactors not using diluent particles show a slightly increased value for  $T_{\text{req}}$  compared to the reactors using diluent. The calculated values for  $T_{\text{req}}$  at a target sulfur level of  $10\text{ mg kg}^{-1}$  are shown in Fig. 6 for reference purposes. The modest difference, at most  $2\text{ °C}$ , would often be classified as "within experimental error". This is not the case

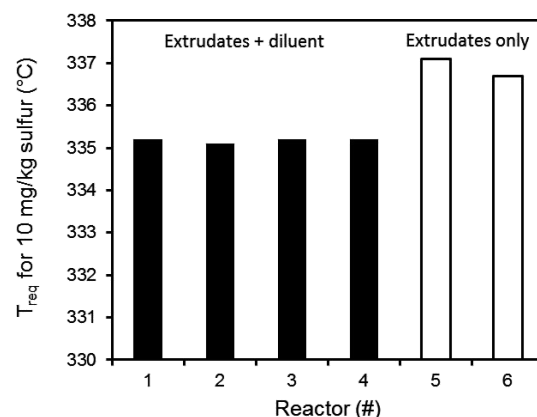


**Figure 6.** Temperature required to achieve a  $10\text{ mg kg}^{-1}$  sulfur level in the product, for reactors using a diluted (1–4) and undiluted bed of extrudates (5 and 6). The activity has been calculated by assuming first-order kinetics for the overall HDS reaction, using an activation energy of  $104.6\text{ kJ mol}^{-1}$ .

here, as the quadruplicate test of diluted extrudates shows a difference no greater than  $0.1\text{ °C}$ , which makes the observed difference in activity between diluted and undiluted extrudates statistically significant. This accuracy is due to the small scale of the experiment and well-defined hydrodynamics – reducing heat effects by optimizing heat transfer [17] and due to the use of parallel reactor technology – reducing typical run-to-run variability compared to single reactors.

## 3.2 Modeling of Data

This section describes the modeling of the experimental results in some detail. Key assumptions made and the theoretical background are also introduced.

### 3.2.1 Mass-Transfer Limitation

In the evaluation it is assumed that external mass transport is not limiting. In earlier work we compared packed-bed microreactors with larger-scale trickle-bed reactors [6]. We found that external diffusion for the model reaction considered (hydrodesulfurization of dibenzothiophene) was not rate limiting in any of the discussed reactors. In view of the fact that this reaction is a slow reaction, this conclusion is not surprising. It should be noted that the sulfur compounds as present in the feedstock used in this study for a large part belong to the category of (substituted) dibenzothiophenes (Fig. 1). The conclusion is corroborated by the observation that the activation energy observed equals  $104\text{ kJ mol}^{-1}$ . This high value does not indicate the presence of external mass-transport limitations.

Mass-transport limitation inside the extrudate particle is not a function of the size or type of the reactor, only the properties of the extrudate particles. For the purpose of the reaction model, the diffusion rate into the extrudate particles is not separately described in the model equations.

### 3.2.2 Axial Dispersion and Plug-Flow Criteria

For kinetic studies, fixed-bed test reactors are usually designed to exhibit flow behavior close to ideal plug flow, such that results can be straightforwardly interpreted based on a plug-flow reactor model [7]. In an ideal plug-flow reactor (PFR), by definition, all reactant molecules have the same residence time in the reactor (same contact time with the catalyst). In reality there is always some degree of dispersion due to diffusion of the molecules in the fluid and the tortuous path of the fluid flow around the solid particles. The net effect is a residence-time distribution for the reactant molecules in the reactor. In general, broadening of the residence-time distribution (larger deviation from plug flow) will lead to a lower reactant conversion than that of the ideal plug-flow reactor.

The deviation from plug flow can be quantified in terms of the dimensionless Peclet ( $Pe$ ) and/or Bodenstein ( $Bo$ ) number. Unfortunately, the definitions of both numbers are often mixed up in the literature. In the present paper, we will stick to the definitions as used by Gierman [18].

$$Pe = \frac{u_0 L_{\text{bed}}}{D}, \quad Bo = \frac{u_0 d_p}{D} \quad (1)$$

As defined in Eq. (1), in which  $u_0$  = superficial gas velocity,  $L_{\text{bed}}$  = catalyst bed length,  $d_p$  = catalyst particle diameter, and  $D$  = dispersion coefficient, the Peclet number measures the magnitude of mass transfer due to convection relative to the mass transfer due to dispersion in the reactor. The higher the Peclet number of a system, the closer it is to ideal plug flow.

For trickle-bed reactors, Gierman proposed the following criterion to ensure less than 10 % deviation from plug flow (in terms of the rate constant one would determine from the experiment using a plug-flow model):

$$Pe > 8n \ln \left( \frac{1}{1-X} \right) \quad (2)$$

in which  $n$  is the order of the reaction and  $X$  the conversion.

For a trickle-bed reactor, the dispersion coefficient  $D$  depends on many factors, including fluid velocities, the flow properties of the fluids (temperature dependent), the diffusivity of the molecules, and the properties of the particle packing. It has been found in experimental studies that data obtained from different systems, under different conditions, can be reconciled in a generalized graph of Bodenstein number versus Reynolds number ( $Re$ ) [7]. Correlations found are typically of the form shown in Eq. (3) [18]:

$$Bo = aRe^b \quad (3)$$

By combining Eqs. (1) and (2) we can write:

$$Pe = \frac{L_{\text{bed}}}{d_p} Bo > 8n \ln \left( \frac{1}{1-X} \right) \quad (4)$$

It can be seen from Eq. (4) that for a fixed-bed system axial dispersion can be minimized by adjusting the ratio of the bed length to particle diameter. This can be achieved by either

increasing the bed length ( $L_{\text{bed}}$ ) or decreasing the particle size ( $d_p$ ). In addition, based on the dependence of the Bodenstein number on the Reynolds number, it can be concluded that axial dispersion will be more pronounced at low fluid velocities. The fluid velocity is directly correlated to the catalyst-bed length at a given value of space velocity and hydrogen-to-oil ratio.

### 3.2.3 Tanks-in-Series Model

To investigate the role of axial dispersion for the string reactor, the experimental results have been interpreted with a tanks-in-series model (TISM). TISM is a simple alternative to the axial dispersion model (ADM), and describes a nonideal reactor as a chain of  $N$  equal-sized CSTRs in series. The number of tanks  $N$  can be related to the Peclet number, based on Eq. (5) [19].

$$Pe = 2(N - 1) \quad (5)$$

By describing the conversion of sulfur as an irreversible, first-order reaction, the TISM leads to Eq. (6) for the sulfur mass fraction in the product ( $S_{\text{prod}}$ ).

$$S_{\text{prod}} = S_{\text{feed}} \left( 1 + \frac{k/LHSV}{N} \right)^{-N} \quad (6)$$

The temperature dependence of the reaction rate ( $k$ ) is calculated according to Eq. (7).

$$k = k_{\text{ref}} \exp \left( -\frac{E_A}{R} \left( \frac{1}{T} - \frac{1}{T_{\text{ref}}} \right) \right) \quad (7)$$

On combining Eqs. (3)–(5), we assume  $N$  to be the following function of the length of the catalyst bed (string of extrudates) and oil flow rate:

$$N = 1 + \alpha(L_{\text{bed}})^{\beta} (\phi)^{\gamma} \quad (8)$$

The approach we took in this work was to estimate the parameters  $\alpha$ ,  $\beta$ , and  $\gamma$ , together with the reaction rate ( $k$ ) and activation energy ( $E_A$ ) from the observed sulfur conversion at different  $LHSV$  and temperature settings.

### 3.2.4 Modeling Results

For this particular application, our experience is that in the range of product sulfur levels from 6 to 500 mg kg<sup>-1</sup> (the relevant range for commercial hydrotreaters [1]) the desulfurization reaction can be adequately described by first-order kinetics. The TISM with first-order kinetics for desulfurization was fitted to all data of reactors 1, 2, 3, 4, 11, and 12 (single strings of extrudates with inert diluent material packed around the extrudates (see Fig. 2)), with product sulfur levels in the range from 6 to 500 mg kg<sup>-1</sup>. This excludes the data of the 7.5 cm beds, as the corresponding product sulfur levels are greater than 500 mg kg<sup>-1</sup>.

The variations of experimental conditions used in these experiments are provided in Tab. 3.

**Table 3.** Experimental conditions used in the modeling of the single-pellet-string data and corresponding model results (a total of 47 data points, including replicates).

Entry	Experimental conditions					Model results		
	$V_{\text{cat}}$ [mL]	$L_{\text{bed}}$ [cm]	$\phi_{\text{oil}}$ [mg min <sup>-1</sup> ]	$LHSV$ [mL <sub>oil</sub> mL <sub>cat</sub> <sup>-1</sup> h <sup>-1</sup> ]	$T$ [°C]	$k/LHSV$ [-]	$N_{\text{CSTR}}$ [-]	$Pe$ [-]
1	0.3	15	3.84	0.87	315	7.7	4	6
2	0.3	15	7.69	1.75	335	7.8	11	21
3	0.3	15	15.38	3.50	335	3.9	39	75
4	0.3	15	15.38	3.50	350	6.4	39	75
5	0.6	30	3.84	0.44	315	15.5	6	10
6	0.6	30	7.69	0.87	315	7.7	19	36
7	0.6	30	15.38	1.75	325	5.5	66	129
8	0.6	30	15.38	1.75	335	7.8	66	129

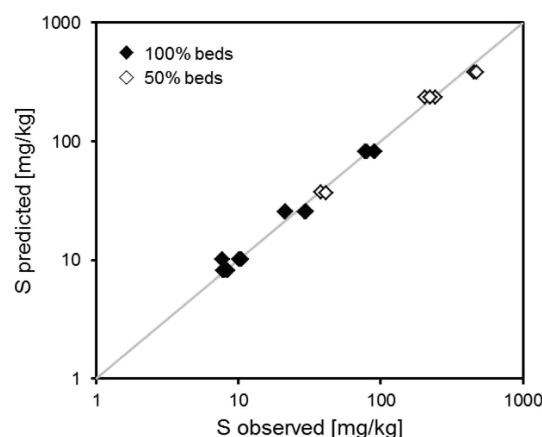
The model parameters (47 data points including replicates, 5 parameters,  $R^2 = 0.99$ ) were determined in Athena Visual Studio [20] using the nonlinear least-squares solver, with logarithmic weighing on the observed product sulfur values. Tab. 4 shows the determined values with 95 % confidence intervals. The corresponding parity plot with predicted versus observed product sulfur, is shown in Fig. 7.

**Table 4.** Determined model parameters and their 95 % confidence intervals (C.I.).

Entry	Parameter	Value	95 % C.I.
1	$k_{\text{ref}}$ (335 °C) [mL <sub>oil</sub> mL <sub>cat</sub> <sup>-1</sup> h <sup>-1</sup> ]	13.6	±0.3
2	$E_A$ [kJ mol <sup>-1</sup> ]	104.1	±2.8
3	$\alpha$ [-]	10.3	±2.0
4	$\beta$ [-]	0.78	±0.2
5	$\gamma$ [-]	1.9	±0.2

The value found for the activation energy is in the expected range of 100–130 kJ mol<sup>-1</sup> [1]. Based on Eq. (4), the value for  $\beta$  was expected to be around 1; the value estimated from the data is lower, but still in the 99 % confidence interval.

The determined deviations from ideal plug flow can be visualized in a graph of the measured product sulfur versus  $k/LHSV$  (Fig. 8). The added lines correspond to the model (Eq. (6)) for different numbers of tanks in series (solid lines) and an ideal plug-flow reactor (dotted line). From the values in Tab. 3 it can be seen that the oil flow rate has a stronger effect on the Peclet number than the length of the string reactor in the investigated range. The two points in Fig. 8 that deviate most correspond to the lowest oil-flow setting. To highlight the impact of oil flow rate, consider also Fig. 9. Plotted here are the HDS reaction rates that would have been determined from the tested conditions, assuming ideal plug flow (normalized to 335 °C), as a function of the oil flow rate. The reaction rate is calculated using Eq. (9).

**Figure 7.** Parity plot comparing the sulfur content predicted by the model against the sulfur content observed experimentally. The solid line represents the theoretical exact match, for which the observed and predicted sulfur contents are identical. The degree of deviation from this ideal line indicates the error of prediction, which is small in this case.

$$k_{\text{PFR}}(T_{\text{ref}}) = LHSV \ln \left( \frac{S_{\text{feed}}}{S_{\text{prod}}} \right) \exp \left( \frac{E_A}{R} \left( \frac{1}{T} - \frac{1}{T_{\text{ref}}} \right) \right) \quad (9)$$

At the highest flow rate,  $k_{\text{PFR}}$  is close to the value of 13.6 fitted with the TISM (Tab. 4). At the lower flow rates, lower apparent rates are found. The data at the lowest oil flow rate deviate most, in agreement with the expectation that dispersion will be highest at the lowest flow rate. This observation suggests that the minimal flow rate is around 10 mg min<sup>-1</sup>.

For the demanding application tested here – producing a diesel containing 10 mg kg<sup>-1</sup> sulfur from a feedstock containing 15977 mg kg<sup>-1</sup> of sulfur – the Peclet number should be greater than 59 based on the German criterion. This translates to a minimum of 30 tanks in series to keep the deviation from plug flow below 10 % [18]. From Tab. 3, it can be concluded that for  $LHSV$  values greater than 1 h<sup>-1</sup>, the 30 cm string reactor can be used to operate in the near-ideal plug-flow regime. At lower oil

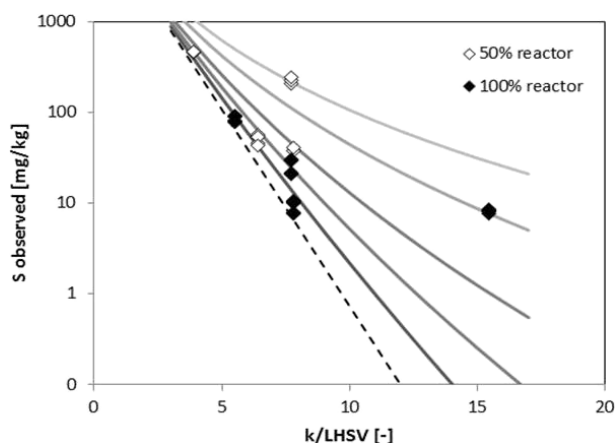


**Figure 8.** Measured sulfur in the product as a function of the rate constant normalized for  $LHSV$  (markers). The dotted line indicates the simulated trend assuming ideal PFR behavior, the solid lines indicate simulated approximations assuming different amounts of CSTRs in series.

flow rates, the deviation from plug flow increases to above 10 %.

### 3.3 Bench-Scale Experiments

From the modeling results it could be concluded that, under the right circumstances, test results from a single-pellet-string reactor are of direct relevance to larger-scale applications. To further explore this feature, a direct comparison has been made between the small-scale results, and test results under similar conditions in a more conventional bench-scale reactor. The feedstock and catalyst were identical, and test conditions were kept comparable as much as possible. The results are shown in Fig. 10.

Despite inherent differences between the design and properties of the two reactors, the correspondence in performance is remarkable. Both the sulfur content and the density of the product, which are key performance indicators for assessing HDS catalyst quality, match up. This implies that an isothermally operated single-pellet-string reactor is an adequate replacement for a larger reactor. Moreover, the obtained accuracy of testing in small-scale parallel reactors offers the opportunity to reliably discriminate between catalysts with even smaller differences.

## 4 Conclusion

In this work, we show that the single-pellet-string reactor (SPSR) is a valid reactor design for evaluating a high-conversion application like hydrodesulfurization (HDS). This

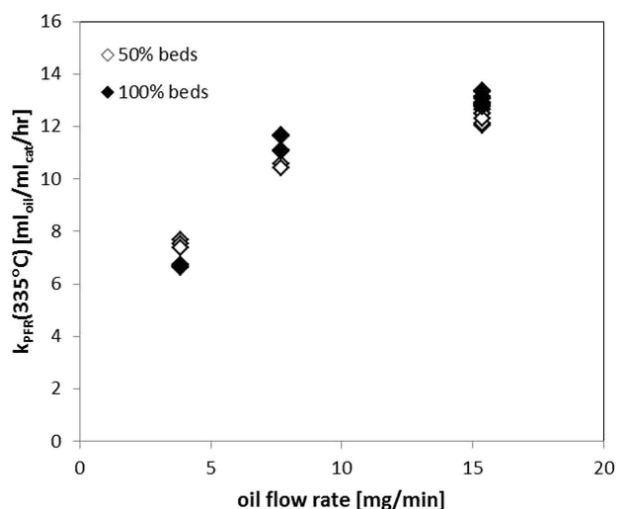


**Figure 9.** Calculated reaction-rate constant based on ideal plug flow as a function of experimentally applied flow rate.

was first demonstrated by exploring a wide variety of experimental conditions in a 16-parallel-reactor setup, for a combination of industrial feedstock and a commercial HDS catalyst. Results obtained are in line with expectation, and even a typical target sulfur level of  $10 \text{ mg kg}^{-1}$  can be achieved at an appropriate temperature. Reproducibility was assessed for this case by means of test replication, and the error between reactors was determined at  $0.1^\circ\text{C}$  at a required temperature of  $335^\circ\text{C}$  to achieve the target sulfur content.

By modeling the obtained results using  $N$  mixers in series model combined with first-order kinetics for the overall HDS reaction, boundary conditions for achieving appropriate performance have been determined. Most importantly, an appropriate catalyst-bed length (and thus superficial velocity) should be applied to limit deviation from ideal plug-flow behavior. A smaller, but also important contribution to idealizing the result was achieved by adding small particulate diluent material surrounding the catalyst extrudates.

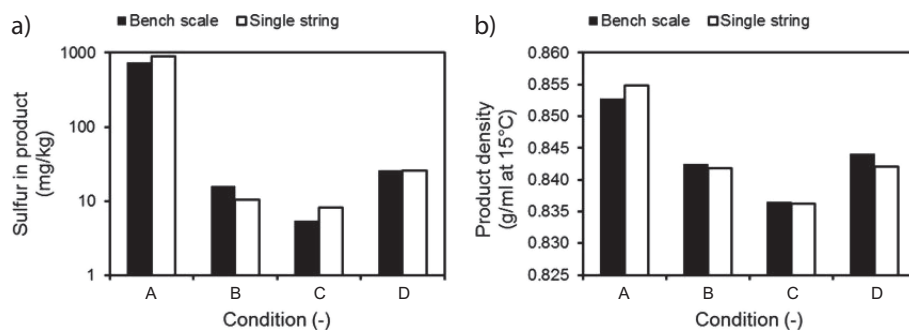


**Figure 10.** Performance comparison between a 225 mL bench-scale reactor and the single-string reactor, which show excellent correspondence for both sulfur in the product (a) and the product density (b). In both reactor setups a pressure of 80 barg and a hydrogen-to-oil ratio of  $500 \text{ Nm}^3 \text{ m}^{-3}$  were applied. Four different combinations of temperature and  $LHSV$  were compared: (A)  $-315^\circ\text{C}$  at  $1.75 \text{ h}^{-1}$ ; (B)  $-335^\circ\text{C}$  at  $1.75 \text{ h}^{-1}$ ; (C)  $-315^\circ\text{C}$  at  $0.5 \text{ h}^{-1}$ ; (D)  $-315^\circ\text{C}$  at  $0.8 \text{ h}^{-1}$ . Note that, as can be expected between two reactors of different design, the  $LHSV$  and the time on stream were not matched exactly between the two experiments.



Finally, the results obtained in the SPSR have been compared to those obtained in a more conventional, larger bench-scale reactor using a catalyst volume of 225 mL. Correspondence in key product properties – sulfur content and density – is excellent. Moreover, despite the difference in scale between the two reactor concepts, catalyst activity also corresponds. Loading a single extrudate string reactor has the advantage of well-defined packing, as each of the extrudates is loaded on top of another. This eliminates the risk of a large void sometimes observed in more random packing in bench-scale reactors, and allows for excellent reactor-to-reactor reproducibility, as demonstrated in this research.

The authors have declared no conflict of interest.

## Symbols used

$B_0$	[-]	dimensionless Bodenstein number
$D$	[m <sup>2</sup> s <sup>-1</sup> ]	dispersion coefficient
$d_p$	[m]	catalyst particle diameter
$E_a$	[J mol <sup>-1</sup> ]	activation energy
$FBP$	[°C]	final boiling point
$IBP$	[°C]	initial boiling point
$k$	[mL <sub>oil</sub> mL <sub>cat</sub> <sup>-1</sup> h <sup>-1</sup> ]	reaction rate of hydrodesulfurization reaction
$k_{ref}$	[mL <sub>oil</sub> mL <sub>cat</sub> <sup>-1</sup> h <sup>-1</sup> ]	reaction rate of hydrodesulfurization reaction at reference temperature
$k_{required\ 10\ mg/kg}$	[h <sup>-1</sup> ]	reaction rate to achieve 10 mg kg <sup>-1</sup> sulfur in product
$k_{335\ ^\circ C}$	[mL <sub>oil</sub> mL <sub>cat</sub> <sup>-1</sup> h <sup>-1</sup> ]	reaction rate of hydrodesulfurization reaction at 335°C
$L_{bed}$	[m]	catalyst bed length
$LHSV$	[h <sup>-1</sup> ]	liquid hourly space velocity
$n$	[-]	reaction order
$N$	[-]	number of ideal continuous stirred tanks in series
$Pe$	[-]	dimensionless Peclet number
$R$	[J K <sup>-1</sup> mol <sup>-1</sup> ]	gas constant, 8.314 J K <sup>-1</sup> mol <sup>-1</sup>
$R^2$	[-]	R-squared; coefficient of determination
$Re$	[-]	dimensionless Reynolds number
$S$	[mg kg <sup>-1</sup> ]	mass fraction of sulfur
$T$	[K]	temperature
$T_{ref}$	[K]	reference temperature
$T_{req}$	[°C]	temperature required to achieve target sulfur mass fraction in product
$u_0$	[m s]	superficial gas velocity

$V_{cat}$	[mL]	catalyst bed volume, based on compacted bulk density
$X$	[-]	conversion

## Greek letters

$\alpha$	[-]	fit parameter of power law equation
$\beta$	[-]	fit parameter of power law equation
$\phi_{oil}$	[mg min <sup>-1</sup> ]	liquid feed rate of gasoil to single reactor
$\gamma$	[-]	fit parameter of power law equation

## Subscripts

feed	gasoil feed
product	gasoil product

## Abbreviations

ADM	axial dispersion model
C.I.	confidence interval
FID	flame ionization detector
GC	gas chromatography
HDS	hydrodesulfurization
ID	inside diameter
LCO	light cycle oil
PFR	plug-flow reactor
RSD	relative standard deviation
SPSR	single-pellet-string reactor
SRGO	straight-run gas oil
TCD	thermal conductivity detector
TISM	tanks-in-series model
ULSD	ultra-low-sulfur-diesel
WABT	weight-average bed temperature

## References

- [1] A. Stanislaus, A. Marafi, M. S. Rana, *Catal. Today* **2010**, *153* (1), 1–68.
- [2] I. Babich, J. A. Moulijn, *Fuel* **2003**, *82* (6), 607–631.
- [3] B. M. Vogelaar, S. Eijssbouts, J. A. Bergwerff, J. J. Heiszwolf, *Catal. Today* **2010**, *154* (3), 256–263.
- [4] F. S. Mederos, J. Ancheyta, *J. Chem. Appl. Catal. Gen.* **2009**, *355* (1), 1–19.
- [5] S. K. Bej, R. Dabral, P. Gupta, *Energy Fuels* **2000**, *14* (3), 701–705.
- [6] B. H. Alsolami, R. J. Berger, M. Makkee, J. A. Moulijn, *Ind. Eng. Chem. Res.* **2013**, *52* (26), 9069–9085.
- [7] R. J. Berger, J. Pérez-Ramirez, F. Kapteijn, J. A. Moulijn, *J. Appl. Catal., A* **2002**, *227* (1), 321–333.
- [8] D. van Herk, M. T. Kreutzer, M. Makkee, J. A. Moulijn, *Catal. Today* **2005**, *106* (1), 227–232.
- [9] L. E. Kallinikos, N. G. Papayannakos, *Ind. Eng. Chem. Res.* **2007**, *46* (17), 5531–5535.
- [10] [www.avantium.com/flowrence](http://www.avantium.com/flowrence) (Accessed on August 17, 2017)
- [11] R. R. de Ruiten, M. Bracht, G. J. M. Gruter (Avantium), *European Patent 2263790A3*, **2011**.

- [12] R. H. W. Moonen (Avantium), *World Patent 2012047095A1*, **2012**.
- [13] R. H. W. Moonen (Avantium), *US Patent 20160121291A1*, **2016**.
- [14] M. Smit, G. J. M. Gruter (Avantium), *US Patent 7997297B2*, **2011**.
- [15] P. J. Van den Brink, M. Bracht, B. H. Harji (Avantium), *World Patent 2002092219A1*, **2002**.
- [16] Y. Wang, Z. Sun, A. Wang, *Ind. Eng. Chem. Res.* **2004**, *43* (10), 2324–2329.
- [17] E.-J. Ras, S. Gomez-Quero, *Top. Catal.* **2014**, *57* (17–20), 1392–1399.
- [18] H. Gierman, *Appl. Catal.* **1988**, *43* (2), 277–286.
- [19] I. M. Abu-Reesh, B. F. Abu-Sharkh, *Ind. Eng. Chem. Res.* **2003**, *42* (22), 5495–5505.
- [20] [www.athenavisual.com](http://www.athenavisual.com) (Accessed on 17th of August, 2017)